PERFORMANCE ANALYSIS OF THE QUASI 24-PULSE STATCOM

Francisco da Costa Lopes [1,2], Edson H. Watanabe [2] and Luís G. B. Rolim [2,3]

[1] CEPEL
Av. Horácio Macedo, 354
Cidade Universitária – Ilha do Fundão
21941-911 – Rio de Janeiro – RJ
fcl@cepel.br

[2] COPPE/UFRJ
Programa de Engenharia Elétrica
P.O. Box 68504
21941-972 – Rio de Janeiro – RJ
watanabe@coe.ufrj.br

[3] Escola Politécnica/UFRJ
Departamento de Engenharia Elétrica
P.O. Box 68504
21941-972 – Rio de Janeiro – RJ
rolim@coe.ufrj.br

***Abstract* – This work shows a steady- and dynamic-state analysis of a *quasi* 24-Pulse *Static Synchronous Compensator* – STATCOM. The implementation of a prototype is described and some experimental results are presented showing the injection of controlled reactive current in the electrical grid. By using the simulation program PSCAD/EMTDC, the influences of the AC inductance on the performance in steady state are evaluated. A passive filter to improve AC voltage quality is presented, which is validated by digital simulations. An open loop analysis was realized and it was shown the influence of the AC inductance and the DC capacitance on the STATCOM response time. Finally, the influence of the transformers inrush current on DC voltage ripple and non-characteristics harmonics in AC current is analyzed.**

***Keywords* – STATCOM Performance Analysis, *Quasi* 24-Pulse Converter, FACTS.**

I. INTRODUCTION

The STATCOM is a shunt FACTS [1] device that controls the reactive current at the point of common coupling (PCC). It can be applied in transmission lines to increase, in steady state or dynamically, the power transmission capacity. In medium- or low-voltage applications the STATCOM can be used for power factor correction or voltage regulation.

This work focuses on the *quasi* 24-Pulse STATCOM topology that is a multi-pulse STATCOM. This kind of STATCOM uses Pulse Amplitude Modulation (PAM) switching and its arrangement is composed by transformers used in conjunction with inverters so as to synthesize the AC desired voltage at the output terminals.

Multi-pulse STATCOMs are an alternative to PWM STATCOMs. It was shown that in high power applications PWM STATCOMs have more switching and snubbing losses than multi-pulse STATCOMs [2].

Many authors have already analyzed the performance of STATCOM by using mathematical models. Some of them can be applied both to multi-pulse and PWM STATCOMs [3]. Others studies were developed focusing on STATCOM control system in order to investigate or enhance its dynamic response [4][5].

Several studies related to multi-pulse STATCOMs were done [2][5][6][7]. Some of them evaluated the STATCOM behavior under unbalanced voltages [2] or under unbalanced and distorted voltages [8][9]. Others developed a mathematical model involving a *quasi* 24-Pulse STATCOM in order to analyze its transient response [7]. Some works with this STATCOM topology were done so as to validate its operation in power factor correction and voltage regulation [10].

However, a steady- and dynamic-state analysis of the *quasi* 24-Pulse STATCOM has not been done yet. Its DC capacitor and AC equivalent reactor play a crucial role in steady state and dynamic performance and how they affect the performance has not been demonstrated yet.

This work describes the implementation of a *quasi* 24-Pulse STATCOM prototype and shows some experimental results with this equipment injecting controlled reactive current in the electrical grid.

By modeling the STATCOM circuitry in PSCAD/EMTDC simulation program, a performance analysis is done showing the influence of the AC reactor on harmonic contents. It is also shown a passive filter design in order to attenuate the characteristic harmonics on AC voltage and current. An open loop analysis is presented showing the influence of the DC capacitance and AC equivalent reactor values on the response time. Finally, the influence of the transformers inrush currents on the non-characteristics harmonics in AC current is analyzed [11].

II. EXPERIMENTAL STATCOM

A. Experimental Setup

The *quasi* 24-Pulse STATCOM is shown in Fig. 1 with the control system omitted by simplicity. It is composed by four 6-Pulse DC-AC Voltage Source Converters (VSC), one common DC capacitor and four transformers connected in Y-Y and Δ-Y as shown in Fig. 1. The 12-pulse converter formed by VSCs 3 and 4 are driven with a delay of – 15° in respect to the other 12-pulse converter formed by VSCs 1 and 2. This arrangement allows elimination or reduction of some low frequency harmonics components.

The VSCs parameters values are shown in Table 1. The transformers parameters are shown in Table 2. The primary windings are those connected to the VSC side and the secondary windings are connected to the grid. The letter K represents the turn ratio of each transformer. R_{eq} and X_{eq} represent the equivalent resistive losses and leakage reactance, respectively, referred to the secondary side. R_{meq} and X_{meq} are the equivalent core losses referred to secondary side.

An inductor between the converter and the grid is necessary in order to attenuate the harmonic current. Generally the coupling transform is designed in such a way that its leakage inductance performs this function. In absence of the coupling transformer an inductor is included in series with transformer windings. This inductor is the L_T in Fig. 1.

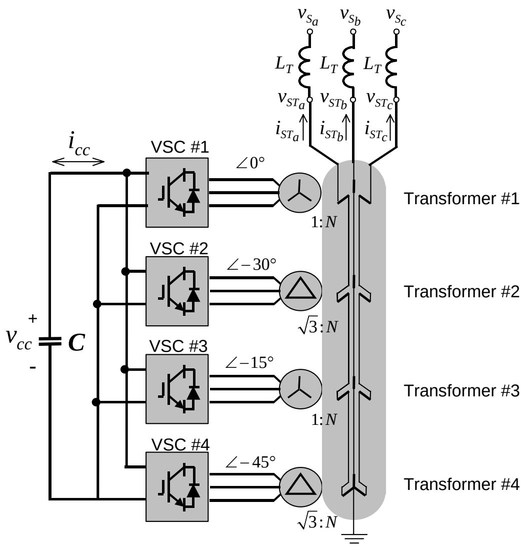

Fig. 1. *Quasi* 24-Pulse STATCOM.

Table 1. Rated parameters of inverters.

Parameter	Individual value	Total value
Power (kVA)	15	60
Line voltage (V)	220	220
Line current (A)	39	39
DC capacitor (μF)	4000	16000

Table 2. Parameters of transformers referred to secondary side.

Transformer #	Primary winding voltage (V)	Secondary winding voltage (V)	K	R_{eq} (mΩ)	X_{eq} (mΩ)	R_{meq} (Ω)	X_{meq} (Ω)
1 (Y-Y)	127	31.75	4	6.2	6.3	32.9	4.0
2 (Δ-Y)	220	31.75	6.9	6.3	5.7	26.8	2.6
3 (Y-Y)	127	31.75	4	6.3	6.1	32.5	3.8
4 (Δ-Y)	220	31.75	6.9	6.3	6.0	25.7	2.5

The basic control system block diagram of the experimental STATCOM is shown in Fig. 2. It was implemented in a microcontroller model SH7047 from Hitachi Micro Systems [12].

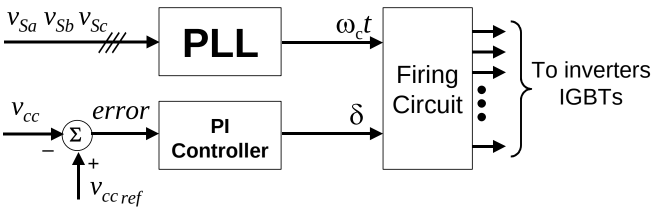

Fig. 2. Control system of experimental STATCOM.

The PLL [13] receives as inputs the three-phase supply voltages v_{Sa}, v_{Sb}, and v_{Sc} and produces the signal $\omega_c t$, which is the instantaneous phase of the grid voltages.

Since reactive power depends on the AC voltages at terminals of STATCOM and these voltages are proportional to DC voltages, the reactive power can be controlled by using the DC voltage as reference. The measured DC voltage v_{cc} is compared with a reference voltage $v_{cc\,ref}$ and the error signal is applied to a PI controller that produces the power angle δ. This angle adjusts the power flow to or from the DC side in order to provide charging or discharging of DC capacitor, thus making the PAM control.

B. Experimental Results

A step signal to the v_{ccref} input that ranges from 250 V to 310 V was applied as shown in Fig. 3. This voltage change makes the STATCOM go from 2 kvar (inductive) to - 2 kvar (capacitive), respectively. This result was obtained with L_T equal to 2 mH. In this situation the response is very slow, as can be seen in Fig. 3.

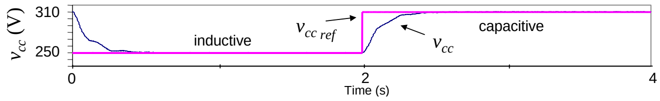

Fig. 3. Step response of DC voltage.

Fig. 4 shows the voltages and currents in steady state when the STATCOM presents an inductive behavior. In this case the STATCOM voltage is smaller than the grid voltage and the current lags the voltage.

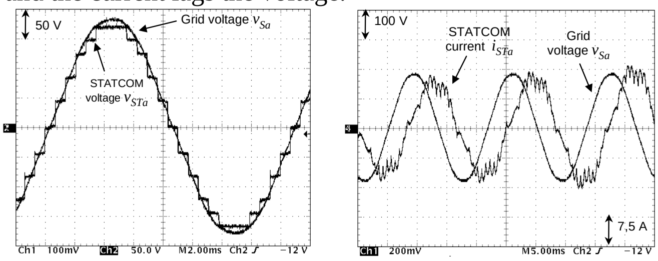

(a) STATCOM and grid voltages. (b) STATCOM current and grid voltage.

Fig. 4. STATCOM voltages and currents – inductive behavior.

Fig. 5 shows the situation where the STATCOM presents a capacitive behavior. The STATCOM voltage is greater than the grid voltage and the current leads the voltage.

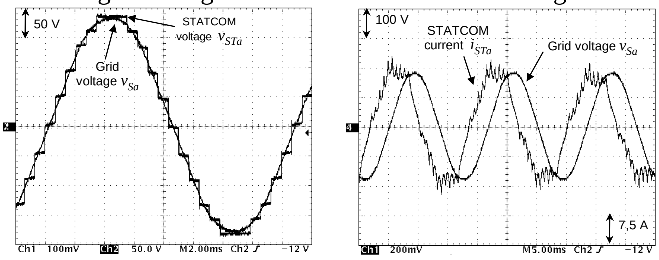

(a) STATCOM and grid voltages. (b) STATCOM current and grid voltage.

Fig. 5. STATCOM voltages and currents – capacitive behavior.

The harmonic contents of the STATCOM voltage are presented in Fig. 6. It can be seen that the major harmonics components are the 23rd and 25th followed by 47th, 49th, 11th and 13th. These harmonic levels are very low in comparison with other converter topologies. For this reason the authors believe that this STATCOM is suitable to many practical applications.

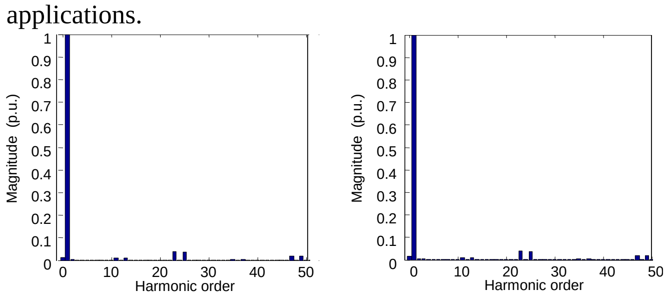

(a) Inductive behavior. (b) Capacitive behavior.

Fig. 6. Harmonic contents of the STATCOM voltage.

III. STEADY STATE ANALYSIS

A. STATCOM Modeling

The STATCOM was modeled in the PSCAD/EMTDC simulation program according to the diagram of Fig. 7. The base values used in the simulations are shown in Table 3.

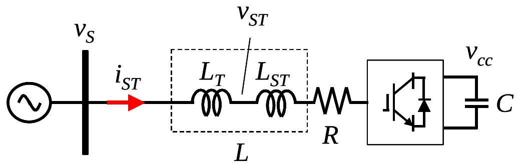

Fig. 7. STATCOM model diagram.

Table 3. Base values used in simulations.

Parameter	Base value
Three-phase power (kVA)	60
Phase to neutral voltage (V)	127
Line to line voltage (V)	220
DC voltage (V)	282.2
Line current (V)	157.5
Impedance (Ω)	0.81

The STATCOM is supposed to be connected to an infinite bus system with negligible inductance. Hence the voltage at point of common coupling (PCC) can be considered equal to the system voltage v_S. The inductance L_{ST} represents the sum of all leakage inductances of STATCOM transformers whose reactances in 60 Hz correspond to X_{eq} values shown in Table 2. Making the calculations, the L_{ST} is equal to 64 μH. The inductance L_T represents the leakage inductance of the coupling transformer or an auxiliary inductor as mentioned before. The sum of these two inductances is represented by L. Naturally, L_{ST} is a fixed value and L_T is the only value that can be changed during simulations.

The resistance R represents all resistive losses in the circuit, which is the sum of the equivalent resistances (R_{eq}) shown in Table 2. The capacitance C represents the sum of all capacitances connected in parallel shown in Fig. 1. The transformer core losses R_{meq} and magnetizing reactance X_{meq} shown in Table 2 also were taken into account in the simulations and were modeled in PSCAD.

The control system used in simulations is based on the p-q Theory [14-16] and is shown in Fig. 8. The instantaneous reactive power q is calculated from the three-phase supply voltages v_{Sa}, v_{Sb}, and v_{Sc} and the three-phase currents i_{STa}, i_{STb}, and i_{STc}. The calculated reactive power q is compared with a reactive power q_{ref} reference and the error signal is applied to a PI controller that produces the power angle δ. The PLL is the same circuit used in experimental STATCOM.

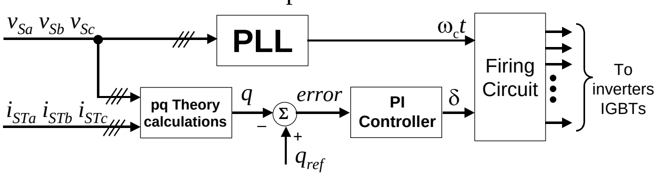

Fig. 8. Control system used in simulations.

B. Influence of the equivalent AC inductance

The simulations were done keeping the reference reactive power fixed at the base value in all cases. By changing the inductance L in each simulation, the Total Harmonic Distortion (THD) of the current i_{ST} was calculated in order to evaluate the influence of the equivalent inductance L on the harmonic contents keeping the DC capacitance value fixed at 16000 μF. The results obtained are shown in Fig. 9.

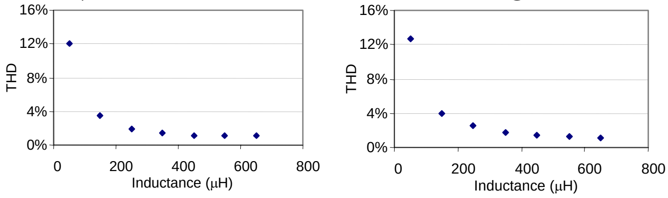

(a) Inductive behavior. (b) Capacitive behavior.

Fig. 9. Relationship between the inductance L and current THD.

This figure shows that the THD decreases drastically with small increases in inductance value. For inductances smaller than 200 μH the STATCOM is inadequate for practical applications due to high harmonic contents injected in the grid.

Since the reactive power of a multi-pulse STATCOM depends on the DC voltage level, this voltage varies in conformity with inductance L in order to keep the reactive power constant at output. Fig. 10 shows how much the DC voltage increases or decreases according to the inductance in order to maintain the reactive power at the base value.

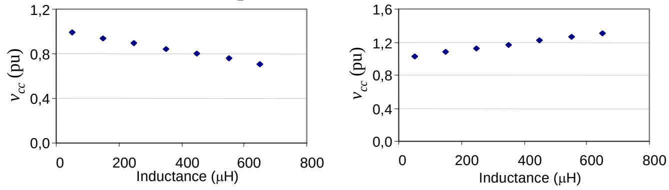

(a) Inductive behavior. (b) Capacitive behavior.

Fig. 10. Relationship between the inductance L and DC voltage.

It can be seen that DC voltage varies linearly with inductance so as to have the same reactive power at STATCOM output terminals. For values greater than 400 μH the DC voltage varies approximately ± 20 % around its base value (1 pu) to produce inductive or capacitive reactive power. Large variation on the DC voltage such as in this case is undesirable because it turns the STATCOM too slow and difficult to control.

C. Passive filter design

In some situations the harmonic current injected in the grid by the STATCOM can be considerably high. In such cases it is necessary to connect a passive filter at the STATCOM AC terminals in order to reduce this harmonic current.

Fig. 11 shows a single-tuned shunt passive filter connected between inductances L_T and L_{ST}. Besides this filter has a resistance inherent to the filter inductance L_F, this resistance is considered negligible in this work. In practical applications this resistance contributes to reduce the attenuation at the resonant frequency. The greater the resistance, the lower is the attenuation at resonant frequency.

The STATCOM is modeled by a voltage source v'_{ST} in series with transformers leakage inductance L_{ST}. The voltage source v_S represents the AC system and the STATCOM terminal voltage is represented by voltage v_{ST}.

By assuming that the voltage v_S has only the fundamental component, it is a short circuit for the harmonic components. Taking this information into account and transforming the circuit variables to Laplace Domain the circuit of Fig. 12 is obtained.

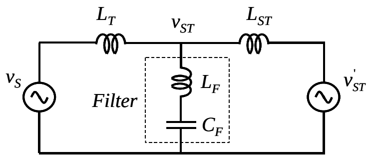

Fig. 11. Passive filter connected at STATCOM terminals.

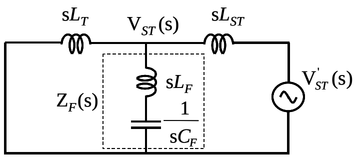

Fig. 12. Equivalent circuit in Laplace Domain.

The resonance frequency of the filter is given by

$$f_r = \frac{1}{2\pi\sqrt{L_F C_F}} . \tag{1}$$

Usually the filter components, that is, L_F and C_F, are calculated in such a way that the resonant frequency of the filter is equal to the harmonic frequency that is to be eliminated. Nevertheless, to accomplish a complete circuit analysis it is important to take into account the other components of the circuit besides L_F and C_F in order to determine how they influence the voltage v_{ST}. This is done by evaluating the transfer function of the filter.

The filter impedance is given by

$$Z_F(s) = sL_F + \frac{1}{sC_F} = \frac{s^2 L_F C_F + 1}{s C_F} \tag{2}$$

and the equivalent impedance given by Z_F and the reactance X_T (= sL_T) is calculated as follows,

$$A(s) = \frac{s^3 L_T L_F C_F + sL_T}{s^2(L_T C_F + L_F C_F) + 1} . \tag{3}$$

Using Fig. 12, the relationship between v_{ST} and v'_{ST} is derived as:

$$V_{ST}(s) = \frac{A(s)}{X_{ST}(s) + A(s)} V'_{ST}(s) \cdot \tag{4}$$

Applying (3) in (4) results in the following equation

$$\frac{V_{ST}(s)}{V'_{ST}(s)} = \frac{s^2(L_T L_F C_F) + L_T}{s^2(L_{ST} L_T C_F + L_{ST} L_F C_F + L_T L_F C_F) + (L_{ST} + L_T)} , \tag{5}$$

that is the transfer function of the filter relating v_{ST} and v'_{ST} .

With this transfer function the gain at high frequencies can be calculated as follows,

$$\left.\frac{V_{ST}(s)}{V'_{ST}(s)}\right|_{s\to\infty} = \frac{L_T L_F}{L_{ST} L_T + L_{ST} L_F + L_T L_F} . \tag{6}$$

For fixed L_T and L_{ST} the high frequencies gain depends only on the filter inductance L_F. To have maximum attenuation at high frequencies L_F must be as small as possible.

For s tending to zero, the low frequencies gain is given by:

$$\left.\frac{V_{ST}(s)}{V'_{ST}(s)}\right|_{s\to 0} = \frac{L_T}{L_{ST} + L_T} . \tag{7}$$

The low frequencies gain depends only on L_T and L_{ST} and the filter capacitance C_F has no influence at both high and low frequencies gains.

The major harmonic component at *quasi* 24-Pulse STATCOM voltage is the 23rd that corresponds to 8671 rad/sec (=23×2π×60 Hz). Applying this value in (1) and choosing L_F equal to 400 μH, then C_F, 33 μF. Applying these values and the values of L_T = 400 μH and L_{ST} = 64 μH in the transfer function shown in (5) the Bode Diagram as shown in Fig. 13 is plotted. This Bode diagram shows negative gain in frequencies other than close to 8671 rad/sec (23rd harmonic).

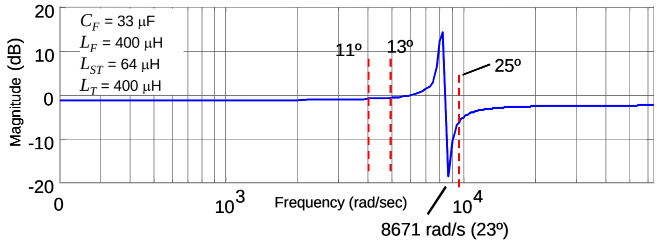

Fig. 13. Bode Diagram of the passive filter.

A simulation with the passive filter connected to the STATCOM was carried out using the same model shown at the beginning of the Section III and the filter components calculated previously. The THD of voltage v_{ST} and current i_{ST} are shown in Table 4 before and after the connection of the filter. Fig. 14 shows the harmonic spectra of the STATCOM voltage v_{ST} before and after the connection of the filter.

Table 4. THD before and after connecting the filter.

THD	Before the connection of the passive filter	After the connection of the passive filter
THD of voltage v_{ST}	5.37 %	3.43 %
THD of current i_{ST}	1.12 %	0.87 %

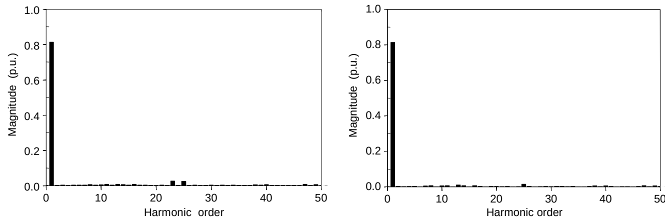

(a) Before connecting the filter. (b) After connecting the filter.

Fig. 14. Harmonic spectra of the STATCOM voltage before and after connecting the passive filter.

Table 4 shows that after the filter was connected the THD of voltage v_{ST} dropped about 50 % and the THD of current i_{ST} dropped about 80 %. Fig. 14 shows that the 23rd harmonic is eliminated and there is an attenuation of other high frequency harmonics too. Therefore the filter designed is suitable to reduce other harmonics components. However the procedure presented here can be carried out to achieve the elimination of other specific harmonic.

IV. DYNAMIC ANALYSIS

A. Open loop analysis - Influence of the AC inductance and the DC capacitance on response time

In this section an open loop analysis is done in order to estimate the STATCOM response time. This analysis is accomplished based on the fact that STATCOM has basically a linear behavior in low frequencies [17]. A step signal is applied in power angle δ input and the reactive power q is measured at the output. By plotting the output signal in a log-plot graph the system order can be investigated [18]. If the curve is a straight line, the system can be considered a first order system. Since the system is a first order one, this chart can be used to estimate the time constant τ of the system that is the time value in the x-axis that corresponds to 36,8 % below the final value in the y-axis.

A simulation study was carried out with L = 264 μH and C = 16000 μF. A known value of power angle was applied at the input at t = 2.5 s and the reactive power measured at the output was plotted in the log-plot graph shown in Fig. 15. The resulting curve is approximately a straight line and in this case the correspondent time constant is 23 ms.

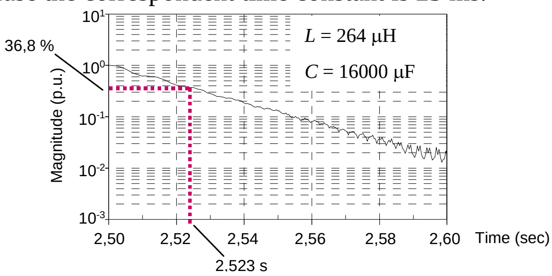

Fig. 15. Response time estimation chart obtained by step response.

To validate this method the frequency response shown in Fig. 16 of the open loop STATCOM was obtained through simulations under the same circumstances. The frequency response reveals that the STATCOM has first order properties that is: (i) the magnitude curve stays constant for low frequencies and after the – 3 dB point the curve decays at 20 dB per decade; (ii) the phase curve shows that for higher frequencies the response tends to – 90°. Further, the time constant can also be obtained through frequency response. It can be demonstrated that the time constant τ is the inverse of the frequency (in rad/sec) at the – 3 dB point [18].

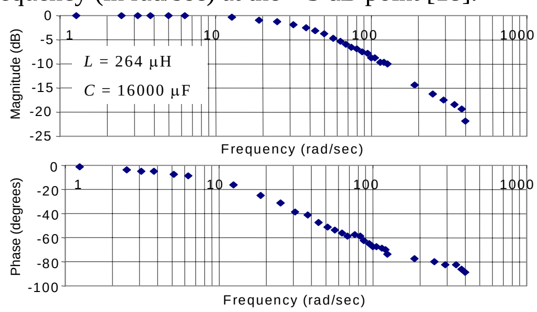

Fig. 16. Open-loop frequency response of reactive power q with respect to the power angle δ input.

Therefore, it is clear that the open loop STATCOM has a first order behavior and the method presented previously can be used to determine the time constant τ. Hence, several simulations in order to determine the influence of the equivalent inductance L and the DC capacitance C on time constant value were carried out. The values obtained for the time constant are shown in Fig. 17 (a) and (b). These figures show clearly that the inductance L has much more influence on the time constant and consequently on the response time, than the DC capacitance.

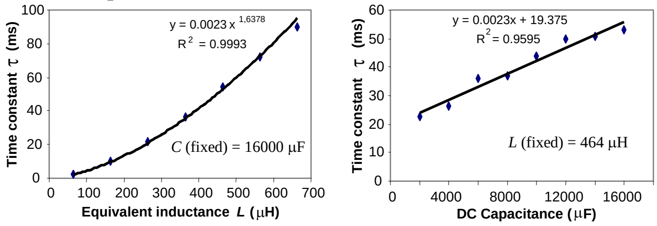

(a) Influence of L on time constant. (b) Influence of C on time constant.

Fig. 17. Influence of the equivalent inductance L and the DC capacitance C on time constant.

B. Non-characteristic harmonics analysis

Since the *quasi*-24 Pulse STATCOM is composed by transformers, an inrush current appears when it is connected to the electric grid. It can be demonstrated that this current has a DC component [19] and this DC level also appears on STATCOM AC current. The DC level on the AC current depends not only on the transformers magnetization reactance and resistance but also on the equivalent inductance L and the equivalent resistance R shown in Fig. 7. Although this DC level tends to zero it can last many cycles. Fig. 18(a) shows the DC level measured from AC current in two STATCOM simulations for two different values of L. It can be seen that the inductance L affects the initial value of DC level and the time to reach zero. Fig. 18 (b) shows the effect of the equivalent resistance R on DC level of AC current. The DC level tends to zero faster when R is five times the transformers equivalent resistance R_{eq}.

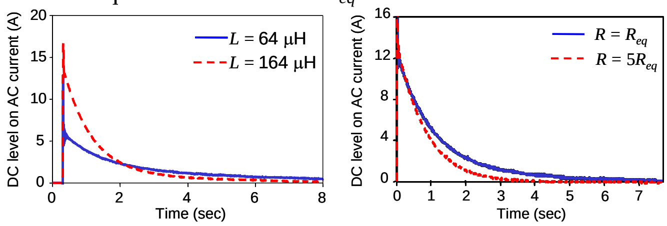

(a) Influence of inductance L on DC level of AC current. (b) Influence of equivalent resistance on DC of AC current.

Fig. 18. Influence of inductance L and equivalent resistance on DC level of AC current.

It can be demonstrated using switching functions that the DC level on the AC current is reflected to the DC voltage v_{cc} as an oscillation at the fundamental frequency [2]. In Fig. 19(a) the simulation result shows how the DC level of AC current affects the voltage v_{cc} causing a ripple on this voltage. It can be seen that the v_{cc} ripple decreases at the same rate that the DC level.

On the other hand, the *quasi* 24-Pulse STATCOM switching function shows that this v_{cc} oscillation is reflected on the AC side as a 2nd harmonic component in the STATCOM current as shown in Fig. 19(b). This non-characteristic harmonic is undesirable and if it is high enough it can damage switching gears and other equipments connected to the grid [19].

Therefore, a temporary resistance should be connected in series with transformers in order to extinguish inrush current and 2nd harmonic in the AC current quickly.

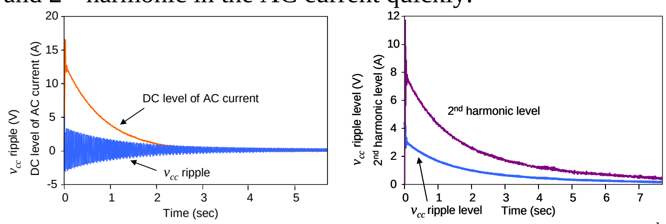

(a) Influence of DC level of AC current on v_{cc} ripple. (b) Influence of v_{cc} ripple on 2nd harmonic.

Fig. 19. Influence of DC level of AC current on v_{cc} ripple and 2nd harmonic.

V. CONCLUSION

This work has shown an analysis of the *quasi* 24-Pulse STATCOM. First, the implementation of a 60 kVA prototype showing its components parts as well as connections and the control system used was presented. Some experimental results were shown with this equipment injecting controlled reactive current into the electric grid. The measured voltage harmonic contents revealed that this equipment is suitable to many practical applications due to low harmonic distortion.

The STATCOM was modeled in the PSCAD program according to the prototype and a steady-state and dynamic analysis were carried out. It was shown that the AC equivalent inductance influences drastically the AC current harmonics and the DC voltage level. A passive filter design was shown in order to attenuate the characteristic harmonics of this STATCOM and simulations were done validating the theoretical calculations.

Using the same digital model a dynamic analysis was done to investigate the STATCOM response time and transient harmonics due to transformers inrush currents. The frequency response revealed that the open loop STATCOM has first order properties. Based on this fact the time constant was obtained and it was concluded that the AC equivalent inductance has more influence on time constant, and consequently on the response time, than the DC capacitance. At last, the effects of the transformers inrush currents on the v_{cc} ripple and on the 2nd harmonic in AC current were shown. In practical applications it is advisable to include a resistance in series with transformers to avoid inrush currents and minimize the non-characteristic harmonics.

REFERENCES

[1] N.G. Hingorani, L. Gyugyi, *Understanding FACTS: Concepts and Technology of Flexible AC Transmission Systems*, IEEE Press, New York, 2000.

[2] C. A. C. Cavaliere, “Análise de STATCOM Operando em Sistemas Desbalanceados”, M.Sc. Dissertation, COPPE/UFRJ, Rio de Janeiro, RJ, Brazil, 2001.

[3] D. Shen, X. Liang, Y. Han, “A Modified Per-unit STATCOM Model and Analysis of Open Loop Response Time”. In: *Proceedings of the IEEE Power Engineering Society Winter Meeting*, Vol. 4, pp. 2624-2629, Singapore, Jan. 2000.

[4] P. W. Lehn, M. R. Iravani, “Experimental Evaluation of STATCOM Closed Loop Dynamics”, *IEEE Transactions on Power Delivery*, Vol. 13, No. 4, pp. 1378-1384, October 1998.

[5] A. H. Norouzi, A. M. Sharaf, “Two Control Schemes to Enhance the Dynamic Performance of the STATCOM and SSSC”, *IEEE Transactions on Power Delivery*, Vol. 20, No. 1, pp. 435-442, January 2005.

[6] S. Bhattacharya, Z. Xi, “STATCOM Operation with Saturable Transformer Under Single Line to Ground Power System Faults”, In: *Proceedings of The Fourth Power Conversion Conference – PCC-Nagoya 2007*, CD-ROM, pp. 975-982, Nagoya, Japan, April 2007.

[7] H. Fujita, S. Tominaga, H. Akagi, “Analysis and Design of a DC Voltage-Controlled Static Var Compensator Using Quad-Series Voltage-Source Inverters”, *IEEE Transactions on Industry Applications*, Vol. 32, No. 4, pp. 970-978, July/August 1996.

[8] D. Shen, W. Liu, Z. Wang, “Study on the Operation Performance of STATCOM under Unbalanced and Distorted System Voltage”, In: *Proceedings of the IEEE Power Engineering Society Winter Meeting*, Vol. 4, pp. 2630-2635, Singapore, Jan. 2000.

[9] C. Schauder, H. Mehta, “Vector Analysis and Control of Advanced Static VAR Compensators”, *IEE Proceedings-C Generation, Transmission and Distribution*, Vol. 140, No. 4, pp. 299-306, July 1993.

[10] C. A. C. Cavaliere, E. H. Watanabe, M. Aredes, *et al.*, “Aplicação do STATCOM na distribuição: regulação de tensão e controle de fator de potência”, In: *Anais do V Seminário Brasileiro sobre Qualidade de Energia Elétrica – V SBQEE*, Vol. 2, pp. 545-550, Aracaju-SE, August 2003.

[11] F. C. Lopes, “Análise de Desempenho de STATCOM *quasi* 24 Pulsos”, M. Sc. Dissertation, COPPE/UFRJ, Rio de Janeiro, RJ, Brazil, March 2006.

[12] Informations about Hitachi microcontroller SH7047: http://eu.renesas.com/fmwk.jsp?cnt=sh7047_root.jsp&fp=/products/mpumcu/superh_family/sh7047_series/sh7047_group/

[13] P.G. Barbosa, E.H. Watanabe, *et al*., “Investigação dos Modelos de Circuitos de Sincronismo Baseados na Teoria das Potências Real e Imaginária Instantâneas (p-PLL e q-PLL)”, In: *Anais do XIV Congresso Brasileiro de Automática – CBA 2002*, Vol. 1, pp. 7-13, Natal, RN, Set. 2002.

[14] H. Akagi, Y. Kanazawa, A. Nabae, “Generalized Theory of the Instantaneous Reactive Power in Three-Phase Circuits”, *International Conference on Power Electronics*, Tokyo, 1983.

[15] H. Akagi, Y. Kanazawa, A. Nabae, “Instantaneous Reactive Power Compensator Comprising Switching Devices Without Energy Storage Components”, *IEEE Trans. on Industry Applications*, Vol. IA-20, No. 3, pp. 625-630, May/June 1984.

[16] E. H., Watanabe, R. M. Stephan, M. Aredes, “New Concepts of Instantaneous Active and Reactive Powers in Electrical Systems With Generic Loads”, *IEEE Transactions on Power Delivery*, Vol. 8, No. 2, pp. 697-703, April 1993.

[17] T. M. L. Assis, E. H. Watanabe, L. A. S. Pilotto, “Analysis of Steady State and Dynamic Performance of a Static Synchronous Compensator (STATCOM)”, In: *Proceedings of the International Conference on Power Systems Transients – IPST´01*, Rio de Janeiro, Brazil, June 2001.

[18] K. Ogata, *Modern Control Engineering*, 3rd Ed, New Jersey, Prentice Hall, 1997.

[19] S. J. Chapman, *Electric Machinery Fundamentals*, 2nd Ed, New Jersey, McGraw-Hill, 1991.